



1 **Multiphase Reaction of SO₂ with NO₂ on CaCO₃ Particles. 2. NO₂-initialized Oxidation of SO₂ by**

2 **O₂**

3 Ting Yu^{1,2,*}, Defeng Zhao^{1,2,*}, Xiaojuan Song^{1,2}, Tong Zhu^{1,2}

4 ¹SKL-ESPC, College of Environmental Sciences and Engineering, Peking University, Beijing, 100871, China

5 ²BIC-ESAT, College of Environmental Sciences and Engineering, Peking University, Beijing, 100871, China

6 *These authors contributed equally to this work.

7 *Correspondence to:* Tong Zhu (tzhu@pku.edu.cn)

8 **Abstract.** The reaction of SO₂ with NO₂ on the surface of aerosol particles has been suggested to be
9 important in sulfate formation during severe air pollution in China. However, we found that the direct
10 oxidation of SO₂ by NO₂ was slow and might not be the main reason for sulfate formation in ambient
11 air. In this study, we investigated the multiphase reaction of SO₂ with NO₂ on single CaCO₃ particles in
12 synthetic air, i.e., in the presence of O₂, using Micro-Raman spectroscopy. The reaction converted the
13 CaCO₃ particle to the Ca(NO₃)₂ droplet containing CaSO₄•2H₂O solid particles embedded in it, which
14 constituted a large fraction of the droplet volume at the end of the reaction. Compared with the reaction
15 in the absence of O₂, the morphology of the particle during the reaction in synthetic air was significantly
16 different and the amount of sulfate formed at the end of the experiment was much higher. The reactive
17 uptake coefficient of SO₂ for sulfate formation was on the order of 10⁻⁵, which was two to three orders
18 of magnitude higher than that in the absence of O₂. According to the difference between the reactive
19 uptake coefficient of SO₂ in the absence of O₂ and that in the presence of O₂, we found that in the
20 multiphase reaction of SO₂ with NO₂ in synthetic air, O₂ was the main oxidant of SO₂ and necessary for
21 radical chain propagation. NO₂ acted as the initializer of the radical formation but not the main oxidant.
22 Such synergy of NO₂ and O₂ resulted in much faster sulfate formation than when either of them was
23 absent. We estimated that the multiphase oxidation of SO₂ by O₂ in the presence of NO₂ can be an
24 important source of sulfate and sink of SO₂ based on the calculated lifetime of SO₂ regarding the loss by
25 the multiphase reaction versus the lifetime regarding the loss by the gas phase reaction with OH radical.
26 Parameterizing the reactive uptake coefficient of the reaction observed in our laboratory for further
27 model simulation is needed, as well as an integrated assessment based on field observation, laboratory
28 study results, and model simulation to evaluate the importance of the reaction in ambient air during the
29 severe air pollution period, especially in China.



30 1 Introduction

31 Multiphase or heterogeneous oxidation of SO₂ by NO₂ has been suggested to potentially play an
32 important role in sulfate formation in the atmosphere (Seinfeld and Pandis, 2006). Recently the
33 multiphase oxidation of SO₂ by NO₂ has been introduced in air quality model simulation to explain the
34 discrepancy between the modeled and observed sulfate concentration during the heavily polluted
35 episodes frequently occurring in China (Cheng et al., 2016; Gao et al., 2016; Wang et al., 2016; Xue et
36 al., 2016), despite the different opinions about the pH value of aerosol particles in China (Wang et al.,
37 2016; Cheng et al., 2016; Liu et al., 2017; Guo et al., 2017).

38 Quantitative and accurate assessment of the role of multiphase oxidation SO₂ by NO₂ on particle
39 relies on determining reaction kinetic parameters and understanding the reaction mechanism. The
40 aqueous oxidation of SO₂ (S(IV) species including H₂SO₃, SO₃²⁻, and HSO₃⁻) by NO₂ has been
41 investigated by a number of laboratory studies (Nash, 1979; Lee and Schwartz, 1983; Clifton et al.,
42 1988; Littlejohn et al., 1993; Santachiara et al., 1990, 1993; Shen and Rochelle, 1998; Spindler et al.,
43 2003; Tursic et al., 2001; Huie and Neta, 1986) and valuable kinetic parameters and understanding on
44 reaction products and process have been obtained. For example, Lee and Schwartz (1983) and Clifton et
45 al. (1988) measured the second order rate constant of the reaction of NO₂ with bisulfate and sulfite
46 solution. The reaction products observed include nitrite, sulfate, and dithionate (e.g., (Littlejohn et al.,
47 1993; Lee and Schwartz, 1983)). Based on these studies, the reaction mechanism was deduced (Clifton
48 et al., 1988; Spindler et al., 2003; Nash, 1979; Littlejohn et al., 1993; Shen and Rochelle, 1998).

49 Previous studies mainly focused on the reaction in bulk solution. Few studies on the oxidation of
50 SO₂ by NO₂ on aerosol particles have been conducted (Santachiara et al., 1990, 1993). On aerosol
51 particles, water activity of aerosol water, pH, ion strength, presence of other compounds or ions, and the
52 role of particle surface are different from dilute bulk solution and may affect the reaction process and
53 reaction rate. Moreover, many previous studies conducted the experiments either in the absence of O₂ or
54 with low O₂ concentrations. Studies on the potential role of O₂ especially at the concentration levels in
55 ambient air and the potential synergy of NO₂ and O₂ in the reaction are very limited.

56 O₂ is abundant in the atmosphere and may affect the multiphase reaction of SO₂ with NO₂. For
57 example, Littlejohn et al. (1993) found that the oxidation rate of sulfite in the aqueous reaction with
58 NO₂ increases with O₂ concentration (0-5% by volume). The enhancement of SO₂ oxidation rate in the
59 reaction with NO₂ have been also found in the heterogeneous reaction on mineral particle surface when
60 O₂ is present (He et al., 2014). Therefore, further studies of the multiphase reaction of SO₂ with NO₂ on
61 aerosol particles in air are needed in order to determine kinetic parameters and elucidate the mechanism
62 of the reaction.

63 In a companion manuscript (Zhao et al., 2017), we reported the results of the study on the
64 multiphase oxidation of SO₂ directly by NO₂ in N₂ on CaCO₃ particles. We found that the reactive



65 uptake coefficient of SO₂ for sulfate formation due to the oxidation by NO₂ is on the order of 10⁻⁸, and
66 concluded that the oxidation of SO₂ by NO₂ alone could not contribute significantly to sulfate formation
67 in the atmosphere. In this manuscript, we present the results of our study on the multiphase reaction of
68 SO₂ with NO₂ in synthetic air, i.e., in the presence of O₂, on CaCO₃ particles. We quantified the reactive
69 uptake coefficient of SO₂ due to the reaction with NO₂/O₂/H₂O mixture in synthetic air. Based on the
70 observations and literature, we further discussed the reaction mechanism. By comparing with the
71 oxidation of SO₂ by NO₂ in N₂, we highlight the role of O₂ in the multiphase oxidation of SO₂.

72 2 Experimental

73 The experimental setup and procedure used in this study have been described in details in previous
74 studies (Zhao et al., 2017; Zhao et al., 2011; Liu et al., 2008). Here we only provide a brief description.
75 The reaction of SO₂ with NO₂ on CaCO₃ particles was investigated using a flow reactor. SO₂ (2000
76 ppm in high purity N₂) and NO₂ (1000 ppm in high purity N₂) were diluted with synthetic air [20% O₂
77 (high purity grade: 99.999%, Beijing Haikeyuanchang Practical Gas Co., Ltd.), 80% N₂ (high purity
78 grade: 99.999%, Beijing Haikeyuanchang Practical Gas Co., Ltd.)] to 75 ppm. Relative humidity was
79 controlled by regulating the flow rates of reactant gases, dry synthetic air, and humidified synthetic air.
80 More details about the experiment conditions can be found in the companion paper (Zhao et al., 2017).
81 SO₂/NO₂/H₂O reaction mixture in synthetic air reacted with individual CaCO₃ particles deposited on
82 Teflon-FEP film. During the reaction, the particles were *in-situ* monitored via a glass window of the
83 flow reactor using a Micro-Raman spectrometer to obtain microscopic images and Raman spectra. All
84 the experiments were conducted at 298±0.5 K.

85 The amount of the reaction product CaSO₄ was quantified based on Raman peak areas and particle
86 sizes. The details of the method are described in our previous study (Zhao et al., 2017). Briefly, the
87 amount of reaction product CaSO₄ formed was followed as a function of time using Raman peak areas.
88 Raman peak areas were converted to the amount of compound using a calibration curve obtained from
89 pure CaSO₄ particles of different sizes, which were determined according to microscopic image. The
90 reaction rate, that is, sulfate production rate, was derived from the amount of sulfate as a function of
91 time. The reactive uptake coefficient of SO₂ for sulfate formation (γ) was further determined from the
92 reaction rate and collision rate of SO₂ on surface of a single particle.

$$93 \quad \gamma = \frac{d(\text{SO}_4^{2-})}{Z} \quad (1)$$

$$94 \quad Z = \frac{1}{4}cA_s[\text{SO}_2], \quad (2)$$

$$95 \quad c = \sqrt{\frac{8RT}{\pi M_{\text{SO}_2}}}, \quad (3)$$



96 where R is the gas constant, T is temperature, M_{SO_2} is the molecular weight of SO_2 , and c is the
97 mean molecular velocity of SO_2 , A_s is the surface area of an individual particle, and Z is the collision
98 rate of SO_2 on surface of a particle. $\{SO_4^{2-}\}$ indicates the amount of sulfate on the particle phase in mole.
99 The average reaction rate and surface area of particles during the multiphase reaction period were used
100 to derive the reactive uptake coefficient. The period was chosen to start after the induction period when
101 $\sim 10\%$ of final sulfate was formed. $[SO_2]$ indicates the concentration of SO_2 in the gas phase.

102 Besides the reaction of SO_2 with $NO_2/O_2/H_2O$ on $CaCO_3$ particles in synthetic air, in some
103 experiments, we varied the concentrations of O_2 in the carrier gas in order to investigate the effect of O_2
104 concentration on the reaction. In addition, we carried out experiments without NO_2 , on either $CaCO_3$
105 solid particle, or $CaCO_3/Ca(NO_3)_2$ internally mixed particle with $CaCO_3$ embedded in $Ca(NO_3)_2$ droplet
106 in order to elucidate the role of NO_2 in the reaction.

107 3 Results and discussion

108 3.1 Reaction products and particle morphology change

109 Figure 1 shows the Raman spectra of a $CaCO_3$ particle during the multiphase reaction of SO_2 with
110 $NO_2/O_2/H_2O$ on it in synthetic air. The peak at 1087 cm^{-1} is assigned to the symmetric stretching of
111 carbonate ($\nu_s(CO_3^{2-})$) (Nakamoto, 1997). During the reaction, the peak at 1087 cm^{-1} decreased
112 continuously and finally disappeared and some new peaks were observed. The peak at 1050 cm^{-1} is
113 assigned to the symmetric stretching of nitrate ($\nu_s(NO_3^-)$). The peak at 1010 cm^{-1} and 1136 cm^{-1} are
114 assigned to the symmetric stretching ($\nu_s(SO_4^{2-})$) and asymmetric stretching ($\nu_{as}(SO_4^{2-})$) of sulfate in
115 gypsum ($CaSO_4 \cdot 2H_2O$), respectively (Sarma et al., 1998). In addition, after the reaction, a broad
116 envelope in the range of $2800\text{--}3800\text{ cm}^{-1}$ assigned to OH stretching of water was observed. On the top of
117 this envelope, there are two peaks at 3408 cm^{-1} and 3497 cm^{-1} , which are assigned to the OH stretching
118 in crystallization water of $CaSO_4 \cdot 2H_2O$ (Sarma et al., 1998; Ma et al., 2013).

119 During the multiphase reaction with $SO_2/NO_2/O_2/H_2O$ mixture, the $CaCO_3$ particle showed a
120 remarkable change in morphology. The original $CaCO_3$ particle was a rhombohedron crystal (Fig. 2,
121 panel i, a). As reaction proceeded, its edge became smoother and later a transparent droplet layer
122 formed, which had a newly-formed solid phase embed in it (Fig. 2, panel i, d). The size of the new solid
123 grew during the reaction (Fig. 2, panel i, d-f) and it seemed to contain a number of micro-crystals.
124 Raman mapping reveals that the new solid phase consisted of $CaSO_4 \cdot 2H_2O$ (Fig. 2, panel iv), and the
125 surrounding aqueous layer consisted of $Ca(NO_3)_2$ (Fig. 2, panel iii).

126 The particle morphology change shown in Fig. 2 is significantly different from the morphology
127 change in the absence of O_2 (Zhao et al., 2017), where the $CaCO_3$ particle was first converted to a
128 spherical $Ca(NO_3)_2$ droplet and then needle-shaped $CaSO_4$ crystals formed inside the droplet (Zhao et
129 al., 2017). Moreover, the amount of $CaSO_4$ formed in the presence of O_2 was much higher than that in



130 the absence of O₂. CaSO₄ solid particle constituted most of the volume droplet here while in the absence
131 of O₂ the few needle-shaped CaSO₄ crystals formed only constituted a small fraction of the droplet
132 volume.

133 3.2 Reaction process

134 During the reaction, the amounts of carbonate, nitrate, and sulfate were followed as a function of
135 time as shown in Fig. 3. In the beginning of the reaction, carbonate decreased slowly and nitrate and
136 sulfate increased slowly. After a period of induction of around 50 min, the reaction accelerated
137 significantly, leading to a fast consumption of carbonate and production of nitrate and sulfate. Finally,
138 carbonate was completely consumed and nitrate and sulfate leveled off.

139 Figure 3 shows nitrate and sulfate were formed simultaneously during the reaction. This finding is
140 in contrast to the finding in the absence of O₂, where nitrate was formed first and sulfate was essentially
141 formed after the complete conversion of CaCO₃ particle to Ca(NO₃)₂ droplet. Moreover, the time for
142 carbonate to be completely consumed was longer here than that in the absence of O₂ (~120 min vs. ~40
143 min) when other conditions were kept the same.

144 3.3 Reactive uptake coefficient of SO₂

145 The reactive uptake coefficient of SO₂ for sulfate formation (γ) in the reaction of SO₂ with
146 NO₂/O₂/H₂O on CaCO₃ in synthetic air and in O₂/N₂ carrier gas with varied O₂ concentrations is shown
147 in Table 1. γ for the reaction of SO₂ with NO₂ in presence of O₂ (5%-86%) is in the range of 0.35 to
148 1.7×10^{-5} , and is 1.2×10^{-5} in synthetic air. The latter is two to three orders of magnitude higher than that
149 for the reaction in N₂ under similar conditions (Zhao et al., 2017). When other conditions were kept
150 constant, γ increased with O₂ concentration. This indicates that O₂ played a key role in enhancing the
151 oxidation of SO₂.

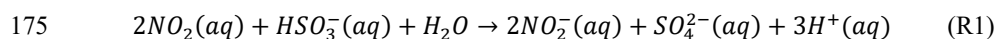
152 The role of O₂ in enhancing the reactive uptake of SO₂ is consistent with the findings in some of
153 previous studies. For example, Littlejohn et al. (1993)'s data show that sulfite oxidation rate increases
154 with O₂ concentration (0-5% by volume). Shen and Rochelle (1998) also found that in the presence of
155 O₂, aqueous sulfite oxidation was enhanced. By investigating the oxidation of SO₂ by NO₂ in
156 mono-dispersed water droplets growing on carbon nuclei, Santachiara et al. (1990) found that sulfate
157 formation rate with 2% O₂ is much higher than that without O₂. Yet, our finding is in contrast to the
158 study by Lee and Schwartz (1983), who found that changing from N₂ to air as carrier gas only increases
159 SO₂ oxidation rate by no more than 10%. The difference between our study and the study by Lee and
160 Schwartz (1983) could be due to the difference in O₂ diffusion from gas to condensed phase and
161 different mechanisms between multiphase reaction on particles and aqueous reaction.

162 **3.4 Reaction mechanism**

163 In the multiphase reaction of SO₂ with NO₂/O₂/H₂O on CaCO₃ particles in synthetic air, we found
164 CaCO₃ could react with NO₂ and H₂O and produce Ca(NO₃)₂, which could deliquesce, forming liquid
165 water, and provide a site for aqueous oxidation of SO₂. This process was similar to the reaction in N₂.
166 The details of this part of the reaction mechanism have been discussed in our previous study (Zhao et al.,
167 2017).

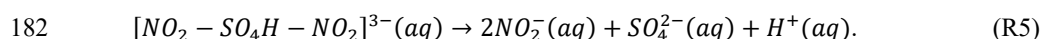
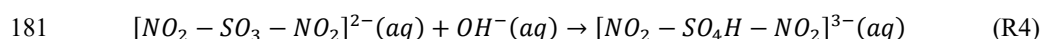
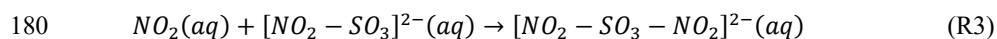
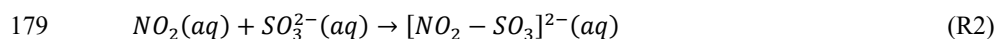
168 Once aqueous phase was formed, SO₂ can undergo multiphase reactions with NO₂/O₂. The detailed
169 mechanism of the aqueous reaction of S(IV) with NO₂ is complex. Previous studies have proposed two
170 different kinds of mechanism. One involves the SO₃⁻ radical formation (Littlejohn et al., 1993; Shen
171 and Rochelle, 1998; Tursic et al., 2001; Spindler et al., 2003) and the other one involves the formation
172 of adduct complexes (Clifton et al., 1988), but not radical formation.

173 In the absence of O₂, Lee and Schwartz (1983) suggest the following reaction equation, according
174 to the reaction products and their yields,

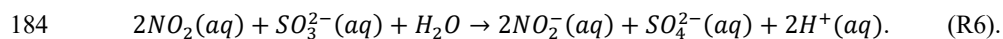


176 The yields of SO₄²⁻, NO₂⁻, and H⁺ relative to the HSO₃⁻ consumed are 1.0±0.05, 1.5±0.4, and
177 2.5±0.4, respectively, and the NO₂⁻ formed relative to NO₂ consumed is 1.0±0.18.

178 Clifton et al. (1988) proposed that the reaction proceeds via NO₂-S(IV) adduct complexes:



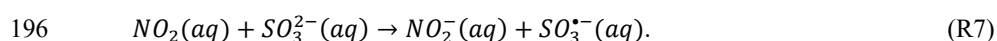
183 By combining reactions R2-R5, the overall reaction equation can be obtained as follows:



185 The reaction R6 is similar to R1.

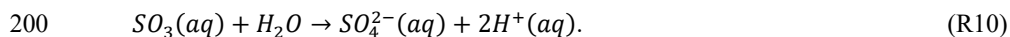
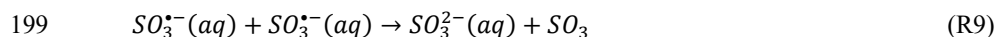
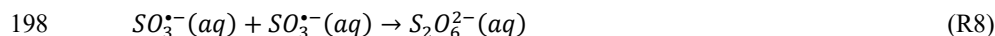
186 If the NO₂-S(IV) adduct mechanism were the main mechanism in this study, there should be no
187 significant difference in the SO₂ oxidation rate between the reaction in the presence of O₂ and in the
188 absence of O₂. In fact, in the presence of O₂ we observed a substantial enhancement in the SO₂
189 oxidation rate compared to the reaction in the absence of O₂. Therefore, the NO₂-S(IV) adduct
190 mechanism is unlikely in this study.

191 In contrast to the adduct complex mechanism, Littlejohn et al. (1993) suggested a radical
192 mechanism. In the reaction of NO₂ with aqueous sulfite, besides SO₄²⁻ and NO₂⁻, they detected S₂O₆²⁻
193 with an appreciable yield using Raman spectroscopy. Since S₂O₆²⁻ is known to be the combination
194 reaction product of SO₃⁻ (Eriksen, 1974; Hayon et al., 1972; Deister and Warneck, 1990; Brandt et al.,
195 1994; Waygood and McElroy, 1992), SO₃⁻ radical is proposed to be formed:



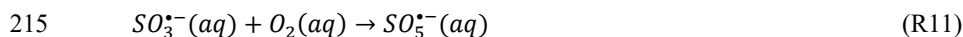


197 $\text{SO}_3^{\cdot-}$ can react via two pathways, forming either $\text{S}_2\text{O}_6^{2-}$ or SO_4^{2-} :

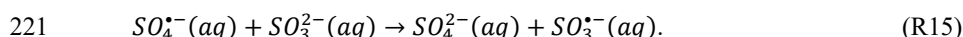
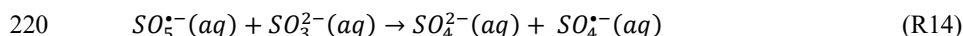
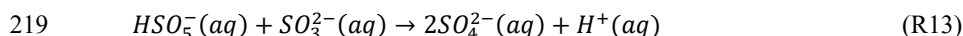
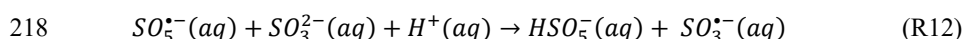


201 The reactions R8-R10 have been well established in the study of the S(IV) oxidation by other
 202 pathways, including the OH oxidation, photo-oxidation, and transitional metal catalyzed oxidation
 203 (Eriksen, 1974; Hayon et al., 1972; Deister and Warneck, 1990; Brandt et al., 1994; Brandt and
 204 Vaneldik, 1995; Waygood and McElroy, 1992). In addition, although previous studies have not reported
 205 the direct observation of $\text{SO}_3^{\cdot-}$ radical in the aqueous reaction of S(IV) with NO_2 , $\text{SO}_3^{\cdot-}$ was directly
 206 observed in the reaction of $\text{NO}_2^{\cdot-}$ with SO_3^{2-} in an acidic buffer solution (pH=4.0) using electron spin
 207 resonance (ESR) (Shi, 1994). Since $\text{NO}_2^{\cdot-}$ is formed in the aqueous reaction of SO_2 with NO_2 and S_2O_6
 208 as the combination reaction product of $\text{SO}_3^{\cdot-}$ is observed (Littlejohn et al., 1993), $\text{SO}_3^{\cdot-}$ formation is
 209 plausible.

210 In the presence of O_2 , Littlejohn et al. (1993) observed that the relative amount of $\text{S}_2\text{O}_6^{2-}$ to SO_4^{2-}
 211 decreases and $\text{S}_2\text{O}_6^{2-}$ is undetectable at low NO_2 concentrations (<5 ppm) in the aqueous reaction of
 212 NO_2 with sulfite. This indicates that O_2 suppresses the reaction pathway of $\text{S}_2\text{O}_6^{2-}$ formation (R8).
 213 Because $\text{SO}_3^{\cdot-}$ radical can react rapidly with O_2 , forming $\text{SO}_5^{\cdot-}$ radical, and thus be consumed, the
 214 suppression of $\text{S}_2\text{O}_6^{2-}$ is readily attributed to the reaction of $\text{SO}_3^{\cdot-}$ with O_2 .



216 Following this reaction, a number of chain reactions can occur and form sulfate (Littlejohn et al.,
 217 1993; Seinfeld and Pandis, 2006; Shen and Rochelle, 1998):



222 The reactions R11-R15 have been well established by the study on the oxidation of S(IV) by OH or
 223 photo-oxidation and all the radicals have been observed (Hayon et al., 1972; Huie et al., 1989; Huie and
 224 Neta, 1987; Chameides and Davis, 1982; Seinfeld and Pandis, 2006).

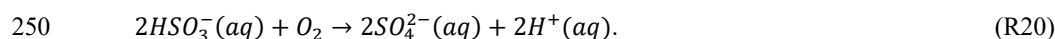
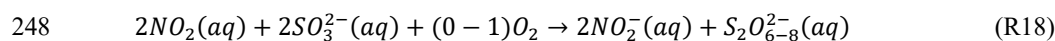
225 The radical mechanism is consistent with the findings of this study and more plausible here. The
 226 enhancement of SO_2 oxidation rate in the reaction of SO_2 with $\text{NO}_2/\text{O}_2/\text{H}_2\text{O}$ with on CaCO_3 particles in
 227 synthetic air compared to that in N_2 can be attributed to the role of O_2 . Although during the reaction in
 228 the absence of O_2 , that is, the direct oxidation of SO_2 by NO_2 , $\text{SO}_3^{\cdot-}$ radical can be formed (R7), the
 229 reaction chain cannot propagate (R11-15). Therefore, the S(IV) oxidation rate and the reactive uptake
 230 coefficient of SO_2 were much lower than that in the presence of O_2 . According to the difference between
 231 the reactive uptake coefficient in the absence of O_2 and in presence of O_2 , the sulfate production rate via
 232 chain reactions due to O_2 (20%) was two to three orders of magnitude faster than the direct oxidation of



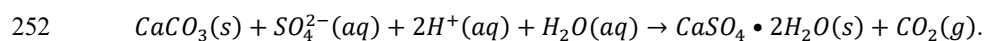
233 SO₂ by NO₂. This indicates that sulfate production was largely contributed by O₂ oxidation via the chain
234 reaction pathway, i.e., “auto-oxidation” of S(IV) and O₂ was the main oxidant of SO₂.

235 Although the direct reaction of NO₂ with SO₂ only contributed a very small fraction to sulfate
236 formation, NO₂ played an important role in SO₂ oxidation by initializing the chain reactions via
237 producing SO₃^{·-} radical (R7). In the experiment without NO₂ while keeping other reaction conditions
238 the same, we found that no sulfate was formed after 5 h of reaction. This indicates that O₂ by itself
239 cannot initialize the chain reaction, although it favors chain propagation. Therefore, NO₂ initiated the
240 oxidation of SO₂ by O₂ and it is the synergy of NO₂ and O₂ that resulted in the fast oxidation of SO₂
241 forming sulfate in this study. Without either NO₂ or O₂, the reaction proceeded much slower.

242 Based on the discussion above, we summarize the reaction mechanism of this study in Table 2. The
243 reactions are classified as chain initiation, chain propagation, and chain termination. Due to the rapid
244 inter-conversion between H₂SO₃, HSO₃⁻, and SO₃²⁻, reactions consuming one of these species will result
245 in instantaneous re-establishment of the equilibria between them (Seinfeld and Pandis, 2006). Overall,
246 the reaction can be written as follows, which shows clearly that O₂ was the main oxidant for sulfate
247 formation:



251 Once sulfuric acid was formed, it can further react with CaCO₃, forming CaSO₄:



253 Overall, besides acting as the initializer of the chain reaction, NO₂ contributed to the formation of
254 aqueous phase by the reaction with CaCO₃ forming Ca(NO₃)₂ as discussed above. The aqueous phase
255 provided the site for S(IV) oxidation.

256 As mentioned above, compared with the reaction in N₂, CaCO₃ was consumed slower in the
257 reaction in synthetic air. This difference can be attributed to two reasons. Firstly, the CaSO₄·2H₂O
258 formed in the reaction can cover CaCO₃ surface and partly suppress the diffusion of aqueous ions such
259 as proton and the contact of reactants with CaCO₃ surface, thus reducing CaCO₃ consumption rate.
260 Secondly, compared with the reaction in N₂, a much higher fraction of CaCO₃ was converted to
261 CaSO₄·2H₂O instead of Ca(NO₃)₂ due to the fast production of CaSO₄·2H₂O. Therefore, the volume of
262 Ca(NO₃)₂ droplet was much smaller than that for the reaction in N₂ for a given CaCO₃ particle. Since
263 the uptake rate of NO₂ was proportional to droplet surface and the NO₂ hydrolysis rate is proportional to
264 droplet volume, the production rate of nitric acid from NO₂ hydrolysis and its reaction rate with CaCO₃
265 were reduced. Therefore, the CaCO₃ particle was consumed slower.



266 4 Conclusion and implications

267 We investigated the multiphase reaction of SO₂ with NO₂/O₂/H₂O on CaCO₃ particle in synthetic
268 air. The reaction converted CaCO₃ particle to Ca(NO₃)₂ droplet with CaSO₄·2H₂O particle embedded in
269 it. CaSO₄·2H₂O constituted a large fraction of the droplet volume in the end of the reaction, in contrast
270 to the small fraction of the droplet volume in the absence of O₂. The Ca(NO₃)₂ droplet formed by the
271 reaction of CaCO₃ with NO₂ provided a site for multiphase oxidation of SO₂. Generally, nitrate and
272 sulfate were formed simultaneously. The reactive uptake coefficient of SO₂ for sulfate formation in the
273 reaction of SO₂ with NO₂/O₂ in synthetic air was determined to be around 10⁻⁵. Compared with the
274 reaction of SO₂ with NO₂ on CaCO₃ particle in N₂, that is, the direct oxidation of SO₂ by NO₂, sulfate
275 production rate was enhanced by around two to three orders of magnitude in the presence of O₂. SO₂
276 oxidation likely proceeded via a chain reaction mechanism according to the findings of this study and
277 literature. O₂ was the main oxidant of SO₂ and NO₂ mainly acted as an initializer of the chain reactions.
278 The synergy of NO₂ and O₂ resulted in fast oxidation of SO₂. Absence of either NO₂ or O₂ led to much
279 slower SO₂ oxidation.

280 Using a method used in our previous study (Zhao et al., 2017), we assess the importance of the
281 multiphase reaction of SO₂ with NO₂/O₂/H₂O by estimating the lifetime of SO₂ due to multiphase
282 reactions and the lifetime due to the gas phase reaction (with OH radical). The lifetime of SO₂ due to
283 the multiphase reaction of SO₂ with NO₂/O₂ is estimated to be around 20 days using the reactive uptake
284 coefficient of SO₂ of 1.2×10⁻⁵ and a typical particle surface area concentration for mineral aerosols in
285 winter in Beijing (6.3×10⁻⁶ cm² cm⁻³) (Huang et al., 2015). This lifetime is substantially shorter than the
286 lifetime regarding the direct oxidation of SO₂ by NO₂ (~7000 days)(Zhao et al., 2017), and comparable
287 to the lifetime of SO₂ due to the gas phase reaction with OH (~12 days assuming daytime OH
288 concentration is 1×10⁶ molecule cm⁻³) (Zhao et al., 2017). Therefore, we conclude that the multiphase
289 oxidation of SO₂ by O₂ in the presence of NO₂ is likely an important source of sulfate and sink of SO₂
290 in the ambient atmosphere, and can play a significant role in the sulfate formation in the heavily
291 polluted haze episodes such as those frequently occurring in China. High sulfate concentrations are
292 observed during these haze episodes, but the mechanism of sulfate formation is still not clear. Model
293 simulation often substantially underestimate sulfate (Cheng et al., 2016; Gao et al., 2016; Wang et al.,
294 2016; Zheng et al., 2015a). During the haze episodes, the high concentrations of SO₂ and NO₂ co-exist
295 and relative humidity is often high (Zhang et al., 2014; Wang et al., 2016; Zheng et al., 2015b). Under
296 these conditions, the multiphase oxidation of SO₂ by O₂ in the presence of NO₂ could proceed rapidly
297 forming sulfate. The enhanced sulfate concentration due to multiphase reactions and resulted aerosol
298 water content can further promote the multiphase oxidation of SO₂. The reaction thus proceeds in a
299 self-accelerated way. Therefore, it can contribute significantly to sulfate formation.



300 Further understanding the mechanism of the multiphase reaction of SO₂ with NO₂/H₂O/O₂ in air is
301 important to understand other atmospheric implications besides sulfate formation. The direct oxidation
302 of SO₂ by NO₂ forms NO₂⁻ with a stoichiometry of 1: 1 and can further form HONO under acidic
303 conditions. HONO can evaporate into the atmosphere and is an important source of OH radical. If NO₂
304 were the main oxidant of SO₂ in the multiphase reaction, the reaction would form one HONO for every
305 sulfate formed. Thus the oxidation of SO₂ by NO₂ can simultaneously be an important source of HONO
306 and OH radical and the SO₂ oxidation would be strongly coupled with reactive nitrogen chemistry. Yet,
307 according to the mechanism of this study, NO₂ only acted as an initializer of chain reactions in SO₂
308 oxidation and essentially the entire SO₂ was oxidized by O₂. Therefore, HONO formation per sulfate
309 formed was trivial. The oxidation of SO₂ by O₂/NO₂ is expected to neither be an important source of
310 HONO and OH in the atmosphere nor significantly influence reactive nitrogen chemistry.

311

312 **Acknowledgements**

313 This work was supported by Natural Science Foundation Committee of China (41421064,
314 21190051, 40490265, 91544000) and Ministry of Science and Technology (Grant No. 2002CB410802).

315 **References**

- 316 Brandt, C., Fabian, I., and Vaneldik, R.: Kinetics and mechanism of the iron(III)-catalyzed autoxidation
317 of sulfur(IV) oxides in aqueous-solution - evidence for the redox cycling of iron in the presence of
318 oxygen and modeling of the overall reaction-mechanism, *Inorg. Chem.*, 33, 687-701,
319 10.1021/ic00082a012, 1994.
- 320 Brandt, C., and Vaneldik, R.: Transition metal-catalyzed oxidation of sulfur (IV) oxides.
321 Atmospheric-relevant processes and mechanisms, *Chem. Rev.*, 95, 119-190, 10.1021/cr00033a006,
322 1995.
- 323 Chameides, W. L., and Davis, D. D.: The free-radical chemistry of cloud droplets and its impact upon
324 the composition of rain, *J. Geophys. Res.-Oceans*, 87, 4863-4877, 10.1029/JC087iC07p04863, 1982.
- 325 Cheng, Y. F., Zheng, G. J., Wei, C., Mu, Q., Zheng, B., Wang, Z. B., Gao, M., Zhang, Q., He, K. B.,
326 Carmichael, G., Poschl, U., and Su, H.: Reactive nitrogen chemistry in aerosol water as a source of
327 sulfate during haze events in China, *Sci. Adv.*, 2, 10.1126/sciadv.1601530, 2016.
- 328 Clifton, C. L., Altstein, N., and Huie, R. E.: Rate-constant for the reaction of NO₂ with sulfur(IV) over
329 the pH range 5.3-13, *Environ. Sci. Technol.*, 22, 586-589, 10.1021/es00170a018, 1988.
- 330 Deister, U., and Warneck, P.: Photooxidation of sulfite (SO₃²⁻) in aqueous solution, *J. Phys. Chem.*, 94,
331 2191-2198, 10.1021/j100368a084, 1990.
- 332 Eriksen, T. E.: pH Effects on the pulse radiolysis of deoxygenated aqueous solutions of sulphur dioxide,
333 *Journal of the Chemical Society, Faraday Transactions 1: Physical Chemistry in Condensed Phases*, 70,
334 208-215, 10.1039/f19747000208, 1974.
- 335 Gao, M., Carmichael, G. R., Wang, Y., Ji, D., Liu, Z., and Wang, Z.: Improving simulations of sulfate
336 aerosols during winter haze over Northern China: the impacts of heterogeneous oxidation by NO₂,
337 *Front. Environ. Sci. Eng.*, 10, 16, 10.1007/s11783-016-0878-2, 2016.
- 338 Guo, H., Weber, R. J., and Nenes, A.: High levels of ammonia do not raise fine particle pH sufficiently
339 to yield nitrogen oxide-dominated sulfate production, *Sci. Rep.*, 7, 12109, 10.1038/s41598-017-11704-0,
340 2017.
- 341 Hayon, E., Treinin, A., and Wilf, J.: Electronic spectra, photochemistry, and autoxidation mechanism of
342 the sulfite-bisulfite-pyrosulfite systems. SO₂⁻, SO₃⁻, SO₄⁻, and SO₅⁻ radicals, *J. Am. Chem. Soc.*, 94,
343 47-57, 10.1021/ja00756a009, 1972.
- 344 He, H., Wang, Y., Ma, Q., Ma, J., Chu, B., Ji, D., Tang, G., Liu, C., Zhang, H., and Hao, J.: Mineral
345 dust and NO_x promote the conversion of SO₂ to sulfate in heavy pollution days, *Sci. Rep.*, 4,
346 10.1038/srep04172, 2014.
- 347 Huang, L., Zhao, Y., Li, H., and Chen, Z.: Kinetics of Heterogeneous Reaction of Sulfur Dioxide on
348 Authentic Mineral Dust: Effects of Relative Humidity and Hydrogen Peroxide, *Environ. Sci. Technol.*,
349 49, 10797-10805, 10.1021/acs.est.5b03930, 2015.



- 350 Huie, R. E., and Neta, P.: Kinetics of one-electron transfer-reactions involving ClO₂ and NO₂, *J. Phys.*
351 *Chem.*, 90, 1193-1198, 10.1021/j100278a046, 1986.
- 352 Huie, R. E., and Neta, P.: Rate constants for some oxidations of S(IV) by radicals in aqueous-solutions,
353 *Atmos. Environ.*, 21, 1743-1747, 10.1016/0004-6981(87)90113-2, 1987.
- 354 Huie, R. E., Clifton, C. L., and Altstein, N.: A pulse radiolysis and flash photolysis study of the radicals
355 SO₂, SO₃, SO₄ and SO₅, *Radiat. Phys. Chem.*, 33, 361-370, 1989.
- 356 Lee, Y.-N., and Schwartz, S. E.: Kinetics of oxidation of aqueous sulfur (IV) by nitrogen dioxide, in:
357 *Precipitation Scavenging, Dry Deposition and Resuspension*, edited by: Pruppacher, H. R., Semonin, R.
358 G., and Slinn, W. G. N., Elsevier, New York, 453-466, 1983.
- 359 Littlejohn, D., Wang, Y. Z., and Chang, S. G.: Oxidation of aqueous sulfite ion by nitrogen-dioxide,
360 *Environ. Sci. Technol.*, 27, 2162-2167, 10.1021/es00047a024, 1993.
- 361 Liu, M. X., Song, Y., Zhou, T., Xu, Z. Y., Yan, C. Q., Zheng, M., Wu, Z. J., Hu, M., Wu, Y. S., and
362 Zhu, T.: Fine particle pH during severe haze episodes in northern China, *Geophys. Res. Lett.*, 44,
363 5213-5221, 10.1002/2017gl073210, 2017.
- 364 Liu, Y. J., Zhu, T., Zhao, D. F., and Zhang, Z. F.: Investigation of the hygroscopic properties of
365 Ca(NO₃)₂ and internally mixed Ca(NO₃)₂/CaCO₃ particles by micro-Raman spectrometry, *Atmos.*
366 *Chem. Phys.*, 8, 7205-7215, 2008.
- 367 Ma, Q., He, H., Liu, Y., Liu, C., and Grassian, V. H.: Heterogeneous and multiphase formation
368 pathways of gypsum in the atmosphere, *Phys. Chem. Chem. Phys.*, 15, 19196-19204,
369 10.1039/c3cp53424c, 2013.
- 370 Nakamoto, K.: *Infrared and Raman Spectra of Inorganic and Coordination Compounds Part A*, John
371 Wiley & Sons, New York, 221-247 pp., 1997.
- 372 Nash, T.: Effect of nitrogen-dioxide and of some transition-metals on the oxidation of dilute bisulfite
373 solutions, *Atmos. Environ.*, 13, 1149-1154, 10.1016/0004-6981(79)90038-6, 1979.
- 374 Santachiara, G., Prodi, F., and Vivarelli, F.: SO₂ oxidation in monodisperse droplets grown on carbon
375 nuclei in presence of NO₂, *J. Aerosol Sci.*, 21, S221-S224, 10.1016/0021-8502(90)90224-1, 1990.
- 376 Santachiara, G., Prodi, F., and Vivarelli, F.: Further experiments on SO₂ oxidation rate in monodisperse
377 droplets grown on carbon nuclei in presence of O₂ and NO₂, *J. Aerosol Sci.*, 24, 683-685,
378 10.1016/0021-8502(93)90024-4, 1993.
- 379 Sarma, L. P., Prasad, P. S. R., and Ravikumar, N.: Raman spectroscopic study of phase transitions in
380 natural gypsum, *J. Raman Spectrosc.*, 29, 851-856,
381 10.1002/(sici)1097-4555(199809)29:9<851::aid-jrs313>3.0.co;2-s, 1998.
- 382 Seinfeld, J. H., and Pandis, S. N.: *Atmospheric chemistry and physics: from air pollution to climate*
383 *change*, 2nd ed., John Wiley & Sons, Inc., 2006.
- 384 Shen, C. H., and Rochelle, G. T.: Nitrogen Dioxide Absorption and Sulfite Oxidation in Aqueous
385 Sulfite, *Environ. Sci. Technol.*, 32, 1994-2003, 10.1021/es970466q, 1998.



- 386 Shi, X. L.: Generation of SO_3^- and OH radicals in SO_3^{2-} reactions with inorganic
387 environmental-pollutants and its implications to SO_3^{2-} toxicity, *J. Inorg. Biochem.*, 56, 155-165,
388 10.1016/0162-0134(94)85002-x, 1994.
- 389 Spindler, G., Hesper, J., Bruggemann, E., Dubois, R., Muller, T., and Herrmann, H.: Wet annular
390 denuder measurements of nitrous acid: laboratory study of the artefact reaction of NO_2 with S(IV) in
391 aqueous solution and comparison with field measurements, *Atmos. Environ.*, 37, 2643-2662,
392 10.1016/s1352-2310(03)00209-7, 2003.
- 393 Tursic, J., Grgic, I., and Bizjak, M.: Influence of NO_2 and dissolved iron on the S(IV) oxidation in
394 synthetic aqueous solution, *Atmos. Environ.*, 35, 97-104, 10.1016/s1352-2310(00)00283-1, 2001.
- 395 Wang, G., Zhang, R., Gomez, M. E., Yang, L., Levy Zamora, M., Hu, M., Lin, Y., Peng, J., Guo, S.,
396 Meng, J., Li, J., Cheng, C., Hu, T., Ren, Y., Wang, Y., Gao, J., Cao, J., An, Z., Zhou, W., Li, G., Wang,
397 J., Tian, P., Marrero-Ortiz, W., Secret, J., Du, Z., Zheng, J., Shang, D., Zeng, L., Shao, M., Wang, W.,
398 Huang, Y., Wang, Y., Zhu, Y., Li, Y., Hu, J., Pan, B., Cai, L., Cheng, Y., Ji, Y., Zhang, F., Rosenfeld,
399 D., Liss, P. S., Duce, R. A., Kolb, C. E., and Molina, M. J.: Persistent sulfate formation from London
400 Fog to Chinese haze, *Proc. Nat. Acad. Sci. U.S.A.*, 113, 13630-13635, 10.1073/pnas.1616540113, 2016.
- 401 Waygood, S. J., and McElroy, W. J.: Spectroscopy and decay kinetics of the sulfite radical anion in
402 aqueous solution, *J. Chem. Soc.-Faraday Trans.*, 88, 1525-1530, 10.1039/ft9928801525, 1992.
- 403 Xue, J., Yuan, Z. B., Griffith, S. M., Yu, X., Lau, A. K. H., and Yu, J. Z.: Sulfate Formation Enhanced
404 by a Cocktail of High NO_x , SO_2 , Particulate Matter, and Droplet pH during Haze-Fog Events in
405 Megacities in China: An Observation-Based Modeling Investigation, *Environ. Sci. Technol.*, 50,
406 7325-7334, 10.1021/acs.est.6b00768, 2016.
- 407 Zhang, J. K., Sun, Y., Liu, Z. R., Ji, D. S., Hu, B., Liu, Q., and Wang, Y. S.: Characterization of
408 submicron aerosols during a month of serious pollution in Beijing, 2013, *Atmos. Chem. Phys.*, 14,
409 2887-2903, 10.5194/acp-14-2887-2014, 2014.
- 410 Zhao, D., Song, X., Zhu, T., Zhang, Z., and Liu, Y.: Multiphase Reaction of SO_2 with NO_2 on CaCO_3
411 Particles. 1. Oxidation of SO_2 by NO_2 , *Atmos. Chem. Phys. Discuss.*, 2017, 1-23,
412 10.5194/acp-2017-610, 2017.
- 413 Zhao, D. F., Zhu, T., Chen, Q., Liu, Y. J., and Zhang, Z. F.: Raman micro-spectrometry as a technique
414 for investigating heterogeneous reactions on individual atmospheric particles, *Sci. China Chem.*, 54,
415 154-160, 10.1007/s11426-010-4182-x, 2011.
- 416 Zheng, B., Zhang, Q., Zhang, Y., He, K. B., Wang, K., Zheng, G. J., Duan, F. K., Ma, Y. L., and
417 Kimoto, T.: Heterogeneous chemistry: a mechanism missing in current models to explain secondary
418 inorganic aerosol formation during the January 2013 haze episode in North China, *Atmos. Chem. Phys.*,
419 15, 2031-2049, 10.5194/acp-15-2031-2015, 2015a.
- 420 Zheng, G. J., Duan, F. K., Su, H., Ma, Y. L., Cheng, Y., Zheng, B., Zhang, Q., Huang, T., Kimoto, T.,
421 Chang, D., Poschl, U., Cheng, Y. F., and He, K. B.: Exploring the severe winter haze in Beijing: the



422 impact of synoptic weather, regional transport and heterogeneous reactions, Atmos. Chem. Phys., 15,

423 2969-2983, 10.5194/acp-15-2969-2015, 2015b.

424

425



426 **Table 1.** Reactive uptake coefficient of SO₂ for sulfate formation under 82% RH and different O₂
427 conditions.

NO ₂ /SO ₂ /O ₂ concentration	γ
75 ppm/ 75 ppm/ 86 %	1.7×10^{-5}
75 ppm/ 75 ppm/ 20 %	1.2×10^{-5}
75 ppm/ 75 ppm/ 5 %	3.5×10^{-6}

428



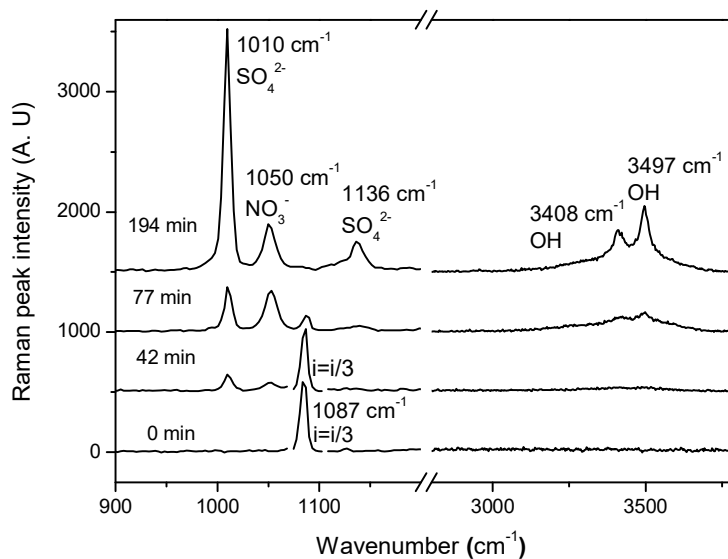
429

430

Table 2. Summary of the mechanism of the reaction S(IV) with NO₂/O₂

Step	Reactions
Initiation	$NO_2(aq) + SO_3^{2-}(aq) \rightarrow NO_2^-(aq) + SO_3^{\bullet-}(aq)$ (R8a)
	$NO_2(aq) + HSO_3^-(aq) \rightarrow NO_2^-(aq) + SO_3^{\bullet-}(aq) + H^+(aq)$ (R8b)
Propagation	$SO_3^{\bullet-}(aq) + O_2(aq) \rightarrow SO_5^{\bullet-}(aq)$ (R11)
	$SO_5^{\bullet-}(aq) + SO_3^{2-}(aq) + H^+(aq) \rightarrow HSO_5^-(aq) + SO_3^{\bullet-}(aq)$ (R12)
	$SO_5^{\bullet-}(aq) + HSO_3^-(aq) \rightarrow HSO_5^-(aq) + SO_3^{\bullet-}(aq)$ (R12b)
	$HSO_5^-(aq) + SO_3^{2-}(aq) \rightarrow 2SO_4^{2-}(aq) + H^+(aq)$ (R13)
	$HSO_5^-(aq) + HSO_3^-(aq) \rightarrow 2SO_4^{2-}(aq) + 2H^+(aq)$ (R13b)
	$SO_5^{\bullet-}(aq) + SO_3^{2-}(aq) \rightarrow SO_4^{2-}(aq) + SO_4^{\bullet-}(aq)$ (R14)
	$SO_5^{\bullet-}(aq) + HSO_3^-(aq) \rightarrow SO_4^{2-}(aq) + SO_4^{\bullet-}(aq) + H^+(aq)$ (R14b)
	$SO_4^{\bullet-}(aq) + SO_3^{2-}(aq) \rightarrow SO_4^{2-}(aq) + SO_3^{\bullet-}(aq)$ (R15)
	$SO_4^{\bullet-}(aq) + HSO_3^-(aq) \rightarrow SO_4^{2-}(aq) + SO_3^{\bullet-}(aq) + H^+(aq)$ (R15b)
	Termination
$SO_3^{\bullet-}(aq) + SO_3^{\bullet-}(aq) \rightarrow SO_3^{2-}(aq) + SO_3$ (R9)	
$SO_3(aq) + H_2O \rightarrow SO_4^{2-}(aq) + 2H^+(aq)$ (R10)	
$SO_4^{\bullet-}(aq) + SO_4^{\bullet-}(aq) \rightarrow S_2O_8^{2-}(aq)$ (R16)	
$SO_5^{\bullet-}(aq) + SO_5^{\bullet-}(aq) \rightarrow S_2O_8^{2-}(aq) + O_2(aq)$ (R17)	

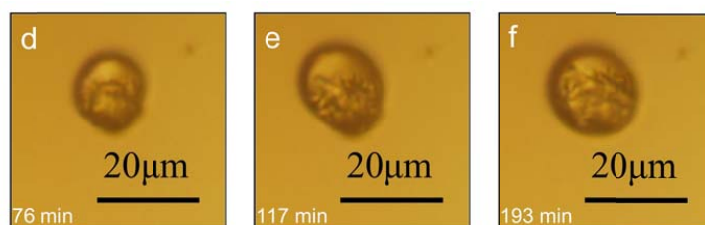
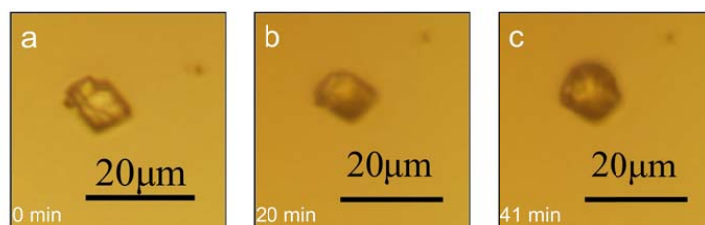
431



432

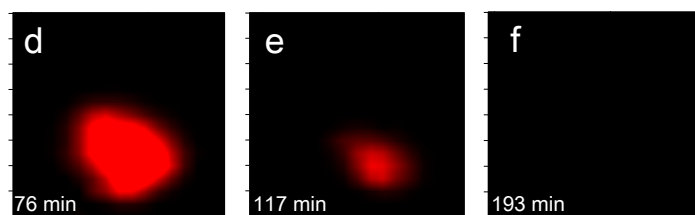
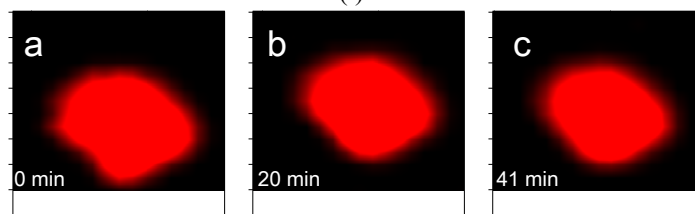
433 Figure 1. Raman spectra of a CaCO₃ particle during the multiphase reaction of SO₂ with NO₂/O₂/H₂O434 on the particle in synthetic air. SO₂: 75 ppm, NO₂: 75 ppm, RH: 72%. The peak intensity of carbonate435 (1087 cm⁻¹) at 0 and 42 min was divided by three for clearness.

436



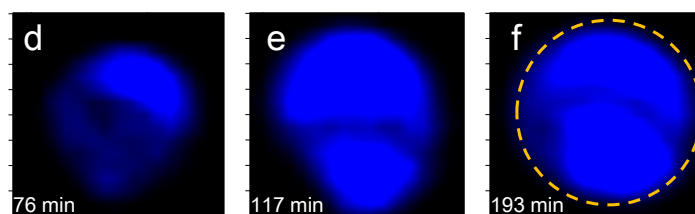
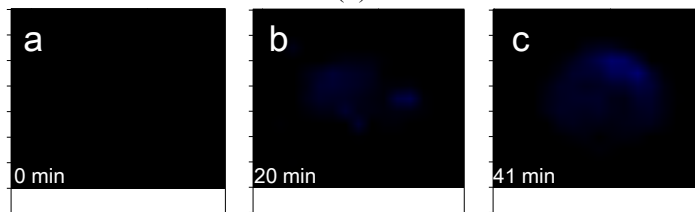
437
438

(i)



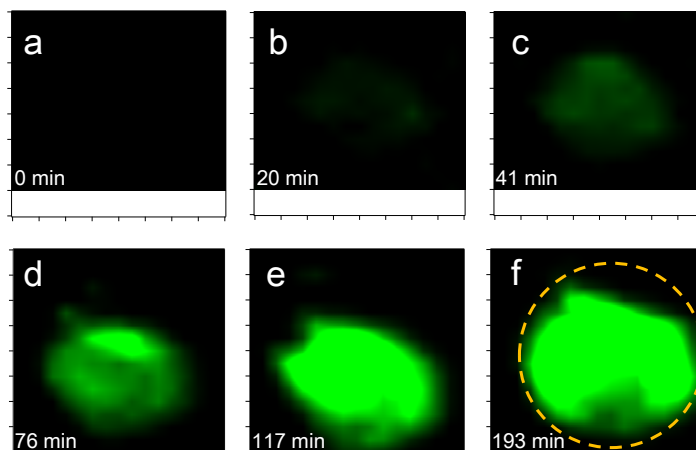
439
440

(ii)



441
442

(iii)



443

444

(iv)

445 Figure 2. Microscopic image (i) and Raman mapping image of carbonate (ii), nitrate (iii), and sulfate (iv)

446 on the CaCO_3 particle during the multiphase reaction SO_2 with $\text{NO}_2/\text{O}_2/\text{H}_2\text{O}$ on the particle in synthetic447 air. A-f corresponds to reaction time of 0, 20, 41, 76, 117, and 193 min. SO_2 : 75 ppm, NO_2 : 75 ppm, RH:

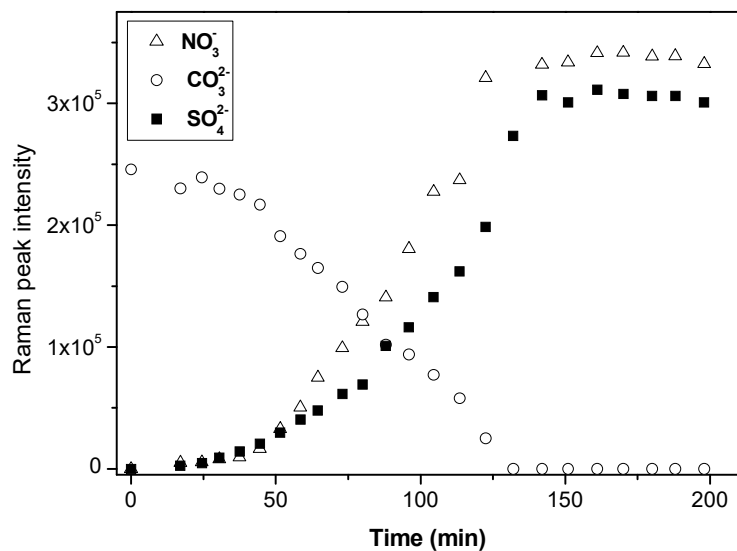
448 72%. The mapping image of carbonate, nitrate, and sulfate are made using the peak area at 1050, 1010,

449 and 1087 cm^{-1} , respectively. The red, blue, and green colors indicate the peak intensity of carbonate,

450 nitrate, and sulfate, respectively. The dashed lines in panel iii-f and iv-f indicate the shape of the droplet

451 at the end of the reaction.

452



453

454 Figure 3. Time series of the Raman peak intensity of the carbonate, nitrate, and sulfate during the
455 reaction of SO_2 with $\text{NO}_2/\text{O}_2/\text{H}_2\text{O}$ on CaCO_3 particles in synthetic air. SO_2 : 75 ppm, NO_2 : 75 ppm, RH:
456 72%. The intensity of NO_3^- , SO_4^{2-} , and CO_3^{2-} show the peak area at 1050, 1010, and 1087 cm^{-1} ,
457 respectively, in Raman spectra obtained by Raman mapping.

458